Design Wave analysis for the M4 wave energy converter

Christine L. Hansen, Hugh Wolgamot, Paul H. Taylor, Jana Orszaghova, Adi Kurniawan, and Henrik Bredmose

***Abstract*—We present physical results for a Design Wave analysis of the M4 wave energy converter (WEC), which is currently being developed for a kW scale deployment in King George Sound, off the coast of Albany, Western Australia. The M4 wave energy converter is a hinged multi-float device utilising relative pitch as the power-producing mode of motion. We have conducted wave basin experiments at the Australian Maritime College in Launceston, TAS Australia, at a scale of 1:15 compared to the ocean trial. We present an experimental analysis of the hinge rotation in a severe sea state identified for the King George Sound location. We identify the most extreme response of the hinge rotation and the wave that causes it – the so-called Design Wave. By averaging the largest structural responses measured in long irregular wave realisations of the extreme sea states, we identify the most likely extreme response. The Design Wave is found to be the average of the surface elevation signals occurring simultaneously with instances of the largest response. The Design Wave thus identified is then produced in the basin and the M4 response measured.**

***Index Terms*—Wave energy converter, Design Wave, Extreme waves, Extreme response**

I. Introduction

EXTREME response statistics for wave energy converters are key in determining the risk of failure. Santo et al. [1] have devised a NewWave-based conditioning model to evaluate the maximum probable response of a structure in a given sea state. The method is widely applicable to structures with predominantly linear responses of interest (see e.g. Grice et al. [2], Zhao et al. [3], [4] or Chen et al. [5]) but was developed for the M4 WEC using an experimentally derived linear response transfer function. The aim of this work is to validate this method by physical experiments for a new configuration of the M4.

This paper presents an experimental Design Wave analysis for the M4 machine. We present key results from extreme wave and Design Wave tests performed as part of a recent laboratory scale experimental campaign conducted at the Australian Maritime College (AMC) at the University of Tasmania. For the first time, we subject the M4 machine to Design Waves, identified through conditioning analysis of long realisations of extreme sea states.

Section I-A and I-B present some background of the M4 WEC and the Design Wave analysis method. Section II then reports on the part of the experiment setup which is relevant to this paper. The results, which are presented in section III, are split into two parts: The analysis leading to identification of the Design Wave sequence is presented in section III-A, and the results from testing the Design Wave in the basin are presented in section III-B. A short discussion of the results and the suggested further work on this topic is included in section IV, and conclusions are given in section V.

A. The M4 wave energy converter

The M4 wave energy converter, developed by M4 Wave Power Limited at the University of Manchester is essentially three rows of cylindrical floats positioned along the direction of wave propagation. The floats are connected by two rigid bodies joined at a hinge, with a total length roughly corresponding to the wavelength of a peak typical wave at the chosen site. This will allow relative pitch motion of the two bodies to drive a PTO system attached to the hinge connecting the bodies. Increasing float diameter and draft from the bow to the stern ensures device alignment with the mean wave direction. A 1-2-1 (1 bow float, 2 centre floats, 1 stern float) float configuration has been chosen for the Albany field scale demonstration project, which is described in more detail in Kurniawan et al. [6], where a linear numerical model and test site wave data are presented.

The forward body consists of three rigidly connected floats arranged with one float at the bow and two at the centre. A hinge is attached at the back of the forward body and the rear body consists of a single float at the stern connected by a rigid frame to the hinge (see Fig. 1 and Fig. 2). The PTO extracts power by acting as a damper of the hinge rotation. During big storms the PTO system is turned off to avoid damage, reducing the damping applied to the hinge rotation.

This work was supported in part by the Australian Research Council (ARC), Early Career Fellowship DE200101478. This research was also supported by Marine Energy Research Australia, jointly funded by The University of Western Australia and the Western Australian Government, via the Department of Primary Industries and Regional Development (DPIRD). The support of the Blue Economy Cooperative Research Centre through the project 'Seeding Marine Innovation in WA with a Wave Energy Deployment in Albany' is gratefully acknowledged. The Blue Economy Cooperative Research Centre (CRC) is established and supported under the Australian Government's CRC Program, grant number CRC-20180101.

Authors C. L. Hansen, H. Wolgamot, P. H. Taylor, J. Orszaghova, A. Kurniawan are with the Oceans Graduate School, University of Western Australia Crawley, WA 6009, Australia and Marine Energy Research Australia MERA. (e-mail: christine.lynggardhansen@research.uwa.edu.au, hugh.wolgamot@uwa.edu.au, paul.taylor@uwa.edu.au, jana.orszaghova@uwa.edu.au, adi.kurniawan@uwa.edu.au)

H. Bredmose is with DTU Wind and Energy Systems, Technical University of Denmark, Kgs. Lyngby 2800, Denmark. (e-mail: hbre@dtu.dk).

Digital Object Identifier:
https://doi.org/10.36688/ewtec-2023-476

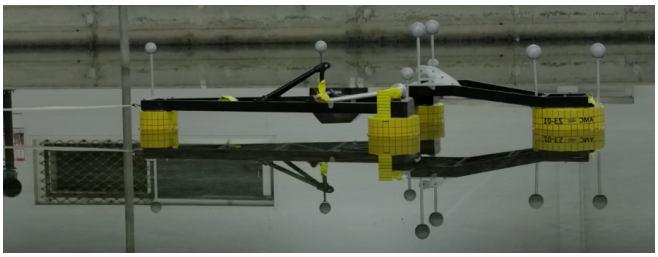

Fig. 1: Photo of the float in calm water with the bow on the left and stern on the right.

Other variants of the device, especially the 1-1-1 and 1-3-2, have been much studied at small scale both numerically and experimentally (e.g. Stansby et al. [7], [8]), and the performance has been evaluated at a range of locations world-wide in Carpinto-Moreno et al. [9] and Orszaghova et al. [10], including in the Southern Ocean off the coast of Albany, WA. Santo et al. [1], [11] evaluated the device in extreme sea states at two locations and found a linear relation between an extreme wave and the hinge rotation response up to about 30°. At this response level, the centre floats were fully submerged – 'dunked' – and water spilled onto the floats, causing significant damping of the response (from estimated up to $\sim 50°$ by a linear model to $\sim 30°$ measured). Collisions between the centre floats and the beam were also observed, an event which could significantly reduce the life span of the device.

B. Design Waves

Design Wave analysis concerns the extreme response of a given structure and identification of the wave event which causes it. Design Waves are short deterministic wave sequences. They have potential to replace long realisations of random waves in low/mid-fidelity numerical models of structural response in long-term extreme response modelling. For development of offshore renewables where cost reduction is key to improve competitiveness, Design Waves used as input to High-fidelity numerical models can help provide detailed insight into nonlinear loads and responses during the largest responses in extreme waves. This can serve as a basis for careful design optimisation.

This section presents the theory associated with linear Design Wave analysis using a conditioning NewWave method. The NewWave, presented by Tromans et al. [12], is a focused wave group corresponding to the average shape of the largest wave in a linear random Gaussian sea state. The concept originated with Lindgren [13] and Boccotti [14], who showed that the average shape of the largest wave in a linear Gaussian sea tends to the scaled auto-correlation function.

The NewWave analysis carried out here, determines the shape and size of the NewWave η^{NW} and the NewResponse of the hinge rotation θ^{NW}. Both signals are determined from realisations of random sea states by extracting and averaging short time segments around the M largest crests in both the surface elevation time series $\eta(t)$ and the corresponding response $\theta(t)$, where $M \ll N$ with N being the total number of crests in the signal.

To understand the relation between the extreme waves and extreme responses, a conditioning process is applied, such that the time intervals corresponding to the extracted crests in $\eta(t)$ are used to construct the averaged response given an incident NewWave (the response conditioned on the NewWave). This signal is denoted the conditioned response and written 'Response|NewWave', or $\theta|\eta^{NW}$. Similarly, the averaged incident wave occurring simultaneously with the NewResponse is written 'Wave|NewResponse' $(\eta|\theta^{NW})$. As θ^{NW} is the averaged largest hinge rotation within the measured sea state, the surface elevation given a NewResponse, $\eta|\theta^{NW}$, is, by definition, the Design Wave.

As the individual crest amplitudes can be assumed to follow a Rayleigh-distribution for a stationary narrow-banded Gaussian random process, we can write the amplitude of the most probable extreme wave or response amplitude, in a given length of time as

$$\alpha_{xN} = \sqrt{2\sigma_x^2 \log N} \tag{1}$$

where σ_x^2 is the variance of signal x and N is the number of crests in the time series. This is well-known, see Newman [15]. The application to both wave and response in the same random sea is discussed in Santo et al. [1]. Applying α for both the surface elevation and response, the NewWave and NewResponse in a unidirectional sea state can be written as

$$\eta^{NW}(t) = \alpha_{\eta N} \frac{\mathrm{Re}\{\sum_n S_\eta(\omega_n)\Delta\omega \exp(-\mathrm{i}\omega_n t)\}}{\sum_n S_\eta(\omega_n)\Delta\omega} \tag{2}$$

$$\theta^{NW}(t) = \alpha_{\theta N} \frac{\mathrm{Re}\{\sum_n S_\theta(\omega_n)\Delta\omega \exp(-\mathrm{i}\omega_n t)\}}{\sum_n S_\theta(\omega_n)\Delta\omega} \tag{3}$$

where ω_n is the angular frequency of spectral components $S_\eta(\omega_n)$ and $S_\theta(\omega_n)$ respectively. The crest focus in time $t_0 = 0$ s and space $x_0 = 0$ m is implicit. As the hinge rotation has been shown to be mostly linear even for large waves in extreme sea states (Santo et al. [1]), a linear transfer function $H(\omega)$ is applied:

$$S_\theta = S_\eta \cdot |H|^2 \tag{4}$$

such that the associated response can be derived from the NewWave:

$$\theta|\eta^{NW}(t) = \alpha_\eta \frac{\mathrm{Re}\{\sum_n S_\eta(\omega_n)\Delta\omega \exp(-\mathrm{i}\omega_n t) \cdot H(\omega_n)\}}{\sum_n S_\eta(\omega_n)\Delta\omega} \tag{5}$$

and the surface elevation conditioned on the response (i.e. the Design Wave), can be written and manipulated as follows

$$\eta|\theta^{NW}(t) = \alpha_\theta \frac{\mathrm{Re}\{\sum_n S_\theta(\omega_n)\Delta\omega \exp(-\mathrm{i}\omega_n t) \cdot H(\omega_n)^{-1}\}}{\sum_n S_\theta(\omega_n)\Delta\omega} \tag{6}$$

$$= \alpha_\theta \frac{\mathrm{Re}\{\sum_n S_\eta(\omega_n) \cdot |H|^2 H(\omega_n)^{-1}\Delta\omega \exp(-\mathrm{i}\omega_n t)\}}{\sum_n S_\theta(\omega_n)\Delta\omega} \tag{7}$$

$$= \alpha_\theta \frac{\mathrm{Re}\{\sum_n S_\eta(\omega_n)\Delta\omega \exp(-\mathrm{i}\omega_n t) \cdot H(\omega_n)^*\}}{\sum_n S_\theta(\omega_n)\Delta\omega} \tag{8}$$

$$\tag{9}$$

where H^* refers to the complex conjugate of the linear transfer function. This implies that phase shifts in $H(\omega_n)$ become negative phase shifts in $H^*(\omega)$. This can be further manipulated to

$$\eta|\theta^{NW} = \frac{\alpha_\theta}{\alpha_\eta}\frac{\sum_n S_\eta(\omega_n)}{\sum_n S_\theta(\omega_n)} \cdot \left(\theta|\eta^{NW}\right)^* \tag{10}$$

which practically means that $\theta|\eta^{NW}$ and $\eta|\theta^{NW}$ are the same shape but with reversed time axes and a constant scale factor between them. This result demonstrates the simple reciprocity which exists between the two signals.

The described method for Design Wave analysis was first used to estimate the average shape of incident waves which excite second order near-trapping modes around a large semi-submersible structure (Grice et al. [2], [16]), but has since been applied for a range of structures and responses e.g. the M4 hinge response by Santo et al. [1], where reciprocity between the Design Wave and associated response was described. Zhao et al. applied NewWave analysis to the run-up on a fixed box [17], for the coupling between roll motion of a barge and sloshing in a tank [4] and in linear and non-linear gap resonance between two barges [3]. Run-up on an FPSO was treated by Chen et al. [18]. For these works, the common denominator is that NewWave analysis has led to determining the averaged shape of Design Waves.

II. Experimental setup

An experimental campaign was carried out in the model test basin at the Australian Maritime College at the University of Tasmania in February 2023 with the aim of obtaining model scale data for the 1-2-1 configuration of the M4 machine prior to the Albany demonstrator deployment. The experiments were carried out at a 1:15 scale relative to the Albany ocean trial. A 3D schematic of the experimental setup is shown in Fig. 2, and a photo of the M4 model is shown in Fig. 1. The waves propagate left to right, and the forward body is positioned on the left side of the photo. The PTO has been taken off for survival sea state tests, and the grey balls placed on top of the structure are used for the QUALISYS optical motion tracking system. The basin is 35 m long and 12 m wide, with 16 piston type wave paddles placed along one short side, and a porous beach with a 1:6 slope along the other. Some key dimensions of the setup are shown in Fig. 3. Note that the basin is longer than it appears in the schematic. The model is placed with its centre line parallel and in the middle between the two side walls. The centre float is placed 9.3 m from the wave maker, and the distance from the model to the beach was ~ 25 m in operating conditions. The model was constructed with fibre glass floats mounted onto carbon fibre frames. For the tests relevant to this survival study, the PTO system was removed and replaced by an equivalent mass attached only to the forward body, thus allowing free rotation. The mooring system consisted of a flexible latex mooring line attached through a force gauge to the bow float and a fixed point in the basin. Cable tension was ensured with a small hanging mass attached by rigid lines and a pulley system to the outsides of both centre floats. A detailed description of the model and the experiment setup is presented in Howe et al. [19].

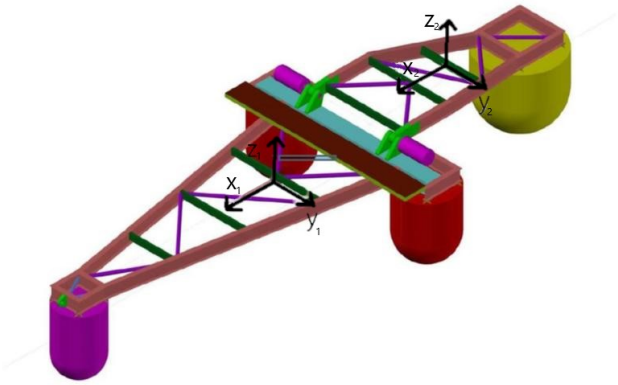

Fig. 2: 3D-schematic of the M4 1-2-1 configuration without power take-off. Rigid-body motion coordinate systems are marked on both bodies.

Sea state variable	AMC Model scale	KGS scale
H_s	0.0680 m	1.02 m
T_p	1.291 s	5 s
γ	1	1
λ_p	2.50 m	37.6 m
h	0.8 m	12 m

TABLE I: Sea state properties for the Australian Maritime College and King George Sound scales

The rigid-body motions in 6 degrees of freedom were captured for both the forward and rear body by the QUALISYS motion-tracking system. Four reflective balls were placed on each body, as seen in Fig. 1. The motion is defined with respect to the local origin of each body. The local motion coordinate systems are defined as shown in Fig. 2, with clockwise rotational motion defined positive, looking in the direction of the axis. The hinge rotation angle θ is defined as

$$\theta = \xi_{5,f} - \xi_{5,r} \tag{11}$$

where $\xi_{5,f}$ and $\xi_{5,r}$ are the local pitch responses of the forward and rear bodies respectively. This convention means that $\theta = 0^\circ$ is the mean position, where the tops of all floats are in line, $\theta < 0^\circ$ corresponds to hinge-down motion and the centre floats sitting below a straight line joining tops of the bow and stern floats, while $\theta > 0^\circ$ corresponds to hinge-up motion and the centre floats sitting above the line joining the tops of the bow and stern floats.

The irregular sea states were calibrated prior to installing the model in the basin, and measured with wave gauges placed at the position of the bow float, between the centre floats and at the stern float, as well as a drift position at 0.6 m behind the stern float. During tests with the model in the basin, surface elevation measurements were taken at the same distance from the wavemaker, but 0.5 m from the basin side wall.

During the experimental campaign, all sea states tested were based on wave data measured in the King

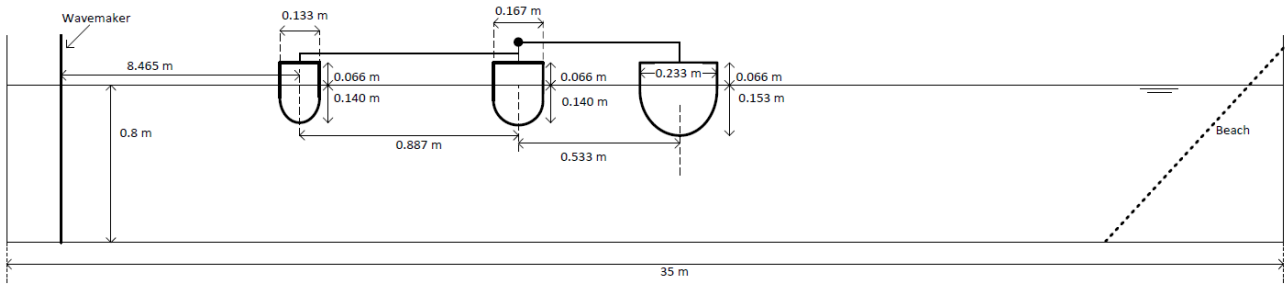

Fig. 3: Simplified side-view schematic of the experiment with some important dimensions. The figure is not to scale, and the basin is longer than it appears.

George Sound. Data was taken from a Spotter wave buoy at the future position of the M4 and an acoustic wave and current profiler at a nearby location in King George Sound. Kurniawan et al. [6] present a joint-probability distribution of significant wave height H_s and zero up-crossing period T_z considering data from the summer months (October-March) over a six-year period. Santo et al. [1] have shown that the response of the M4 device is controlled by the sea state steepness. With respect to the local wavelength λ_z and H_s, the highest measured steepness was:

$$S_s = \frac{H_s}{\lambda_z} = 0.05 \tag{12}$$

For the conditioning analysis, we chose a wave condition along the limiting sea state contour, for which T_p was close to the hinge natural period. The wave spectrum was generated by manual fitting of JONSWAP spectral parameters H_s, T_p and γ to the spectrum of the sea state measured at the site. The spectrum, which was generated based on all 30-minute periods for which the H_s, T_z combination fell within the bounds of the chosen condition in the joint probability table, was initially bimodal with a significant low-frequency swell component, but this was excluded, since the M4 is designed to respond to the local wind-generated waves in King George Sound. The sea state properties are given in model scale and full scale in Table I. A plot of the model scale power spectrum of the incident wave field and the resulting hinge response measured during irregular wave tests at the Australian Maritime college is shown in Fig. 4. It can be seen that the hinge response is relatively narrow-banded around the natural frequency, which is situated within the linear wave range for the extreme sea state. The response spectrum contains both high- and low-frequency second order components, however at much lower levels than the main linear motion.

III. Results

To validate the conditioning NewWave analysis approach to determining the Design Wave for a given response process, we conducted basin experiments in two parts. Firstly, the identified extreme sea state was run for six distinct realisations each with a duration of 25 minutes (1.6 hr field scale). These runs were

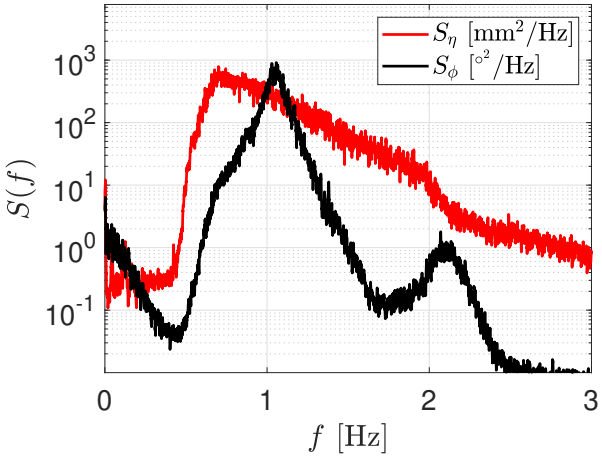

Fig. 4: Power spectrum for the extreme sea state (red) and the hinge response (black) at model basin scale

repeated with and without the model present in the basin, to measure both the surface elevation in the position of the centre floats, and the hinge rotation response to the waves at the same position. The conditioning analysis, as outlined in section I-B, is conducted on the results from this part, as will be described in detail in section III-A. The identified Design Wave signal was then used as the input signal to focused wave group tests, which will be presented and analysed in section III-B.

A. Response conditioning of irregular sea state data

The incident NewWave is found by identifying the M largest crests in the wave and response signals, composed of the six realisations of an irregular sea state with 25 minutes duration each, corresponding to a total 9.7 hours at field scale. We use the $M = 30$ largest crests to create an averaged signal with a long return period and relatively low sensitivity to the variation between the individual crests. A short symmetric time interval is then defined around each crest, and the surface elevation in the M intervals are averaged to produce the incident NewWave η^{NW}, shown in the top subplot in Fig. 5, with the crest occurring at $t = 0$ s. For the conditioning analysis, η^{NW} is now the conditioning signal, in the sense that the time stamps of the intervals

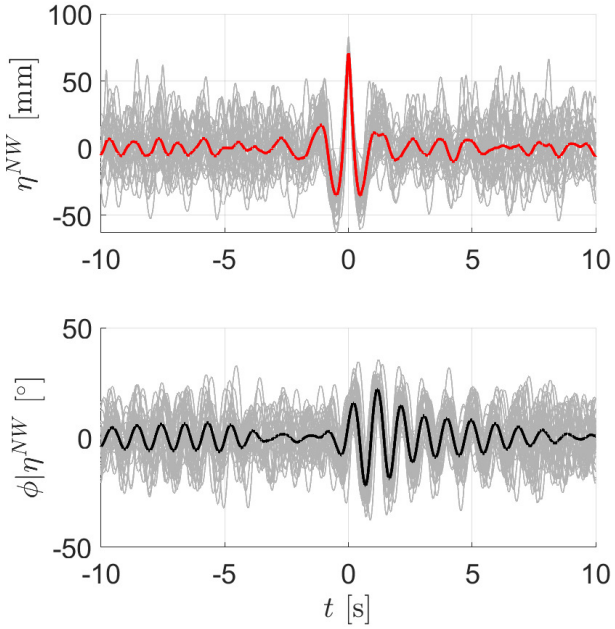

Fig. 5: Top: Conditioning incident NewWave η^{NW} (red) and segments around the 30 largest incident wave crests (grey). Bottom: Associated response $\theta|\eta^{NW}$ (black) and response segments (grey) around the time of occurrence of conditioning incident wave crests.

around each incident wave crest are now applied to the corresponding hinge response signal. Averaging over the M response intervals gives the associated response $\theta|\eta^{NW}$, which is shown in the bottom subplot in Fig. 5. For both η^{NW} and $\theta|\eta^{NW}$, the M time intervals are plotted in grey to demonstrate that all averaged instances converge to the same shape close to $t = 0$ for both signals, but are rather noisy for large $|t|$. This is in agreement with NewWave theory, which tends to the standard deviation of the Gaussian background process for large $|t|$.

The incident NewWave takes the shape of a symmetric narrow wave group with crest amplitude of a similar magnitude to H_s. The associated response is small until close to $t = 0$ s, where the crest of η^{NW} induces large hinge rotation. Subsequently, in the absence of wave forcing in the averaged η^{NW} for $t > 1$ s, the averaged response exhibits a freely decaying motion.

Found through an analogue but reversed process to η^{NW} and $\theta|\eta^{NW}$, the NewResponse θ^{NW} and the corresponding associated incident wave $\eta|\theta^{NW}$ are shown in the top and bottom subplot of Fig. 6 respectively. Given the narrow-banded and highly resonant nature of the hinge response, the NewResponse for the hinge rotation θ^{NW} builds up gradually over at least 5 s and decays slowly. The signal displays clear left-right symmetry, which is an indicator that the effect of nonlinear damping on the response is rather small on average. Local dunking events, where the centre floats are completely submerged, causes local loss of hydrostatic stiffness and substantial energy dissipation [1]. It is assumed that the presence of such events would

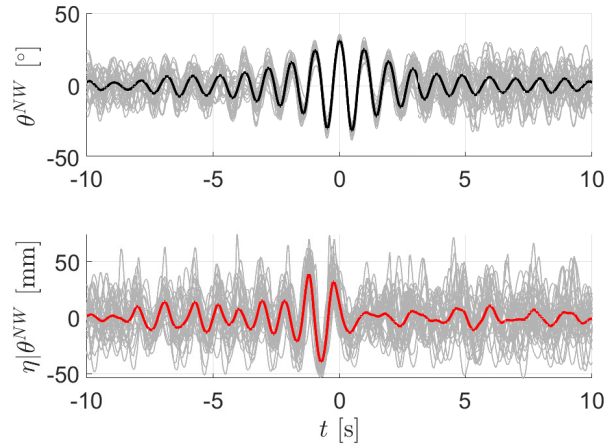

Fig. 6: Top: Conditioning NewResponse θ^{NW} (black) and response segments around the 30 largest response crests (grey). Bottom: Associated incident wave $\eta|\theta^{NW}$ (red) and incident wave segments around the time of occurrence of conditioning response crests (grey).

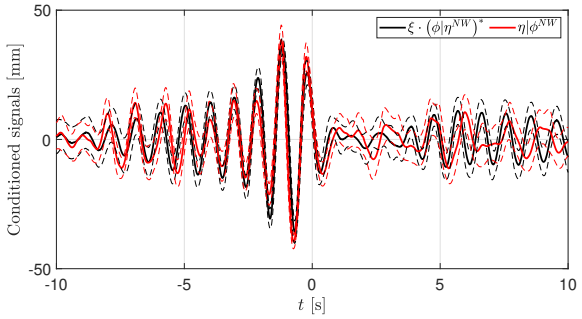

Fig. 7: Reciprocity: time-reversed and scaled response given an incident NewWave (black) and incident wave given a NewResponse (red)

visibly reduce the response amplitude for $t > 0$ s, as they are expected to occur at the largest crest events. Some dunking events have been observed during the irregular wave tests, but it is outside the scope of this work to examine the number of such occurrences within the M largest response crests. One could assume that since dunking reduces the maximum angular displacement of the hinge, the largest 30 response crests might occur in combination with other events which prevent dunking. This is an interesting question, which will be subject to detailed analysis of the wave and response data as well as videos of the run-up on the centre floats during the extreme events.

The associated incident wave – the Design Wave – builds up in amplitude leading up to $t = 0$ s and then drops to values lower than the background noise level at $t > 0$ s, such that the hinge response can decay freely. Comparing $\eta|\theta^{NW}$ and η^{NW}, it is clear that the average of the largest wave of the sea state η^{NW} is very distinct in shape and size from the wave that induces the averaged largest response $\eta|\theta^{NW}$. The maximum amplitude of $\eta|\theta^{NW}$ is ~ 0.5 the crest amplitude of η^{NW}, and the buildup time is long in comparison. The maximum response is $31.1°$ which is 1.41 times the response due to the largest averaged wave.

Fig. 7 shows the incident wave conditioned on the NewResponse $\eta|\theta^{NW}$ and the scaled hinge rotation response conditioned on the incident NewWave $\theta|\eta^{NW}$, mirrored about $t = 0$ s, $\zeta \cdot \left(\theta|\eta^{NW}\right)(-t)$, with the scale coefficient $\zeta = \frac{\sigma_\eta}{\sigma_\theta}$. The dashed lines are error bars defined as $\pm 2\sigma/\sqrt{M}$. The two conditioned signals are very similar in the interval $t = [-7; 7]$ s, which corresponds to the time of the buildup and decay of θ^{NW}.

An interesting difference between the two signals occurs at the beginning of the Design Wave at $t \approx -7$s, where the amplitude suddenly increases followed by a period of 3-4 s, where the amplitude of $\eta|\theta^{NW}$ is relatively constant before again increasing rapidly. At the same time (in Fig. 7) the amplitude of $\theta|\eta^{NW}$ starts visibly smaller than that of $\eta|\theta^{NW}$ and then increases monotonically until it reaches its maximum value. The cause of this difference is not yet understood.

The similarity between the two signals demonstrates that reciprocity, as explained in section I-B, holds and that there is a linear relation between the incident wave and hinge rotation response, even for extreme events within a severe sea state. The scale coefficient ζ acts here as a sort of frequency-averaged relative transfer function.

B. Design Wave experiment results

The Design Wave input signal is produced using the following steps: The wave-signal given a NewResponse $\eta|\theta^{NW}$ is edited by ramping the wave amplitude after $t = 2$ s and eliminating energy after $t = 5$ s and before the beginning of the buildup of the NewResponse θ^{NW}. The Design Wave signal is then elongated with 0-values at each end and propagated back to the position of the paddle ($x_{paddle} = -9.38$ m) in the frequency domain, using linear wave theory, to serve as input to the wave maker software. The Design Wave was run both with and without the M4 device in the basin, and the experimental Design Wave signal is measured at the position of the centre floats without the device installed. The tests were repeated twice with negligible variation.

Fig. 8 shows $\eta|\theta^{NW}$ i.e. the incident wave conditioned on the NewResponse, and the measured Design Wave at the position of the centre float without the model in the basin. The time axis is consistent with that of Fig. 5 and 6, such that the maximum response occurs at $t = 0$ s. The measured Design Wave generally matches the sought input Design Wave in both amplitude, period and phase, albeit the largest measured crest at $t = -1.3$ s is 15% larger than the input Design Wave amplitude. The following crest (at $t = -0.73$ s) and trough (at $t = -0.21$ s) are smaller than the input Design Wave amplitudes, but all three peaks are observed to lie within the $\pm 2\sigma/\sqrt{M}$ error bars for $\eta|\theta^{NW}$ (red dashed lines), and as such the difference is without significance.

The response to the Design Wave is shown with the conditioning NewResponse in Fig. 6. Generally, the measured hinge rotation response to the Design Wave appears in the shape of a NewResponse, and

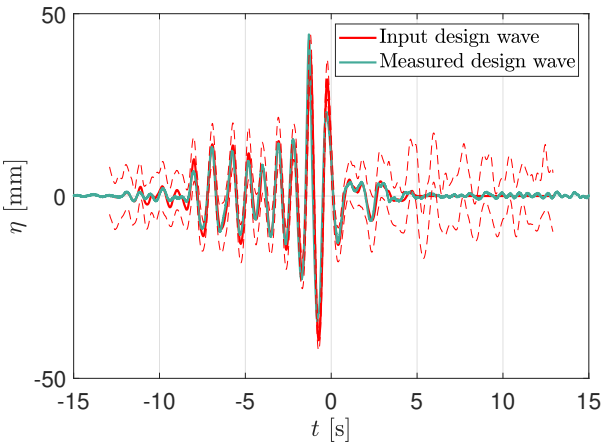

Fig. 8: Input Design Wave (red)with error bars (dashed line, defined as $\pm 2\sigma/\sqrt{M}$) and measured Design Wave (turquoise)

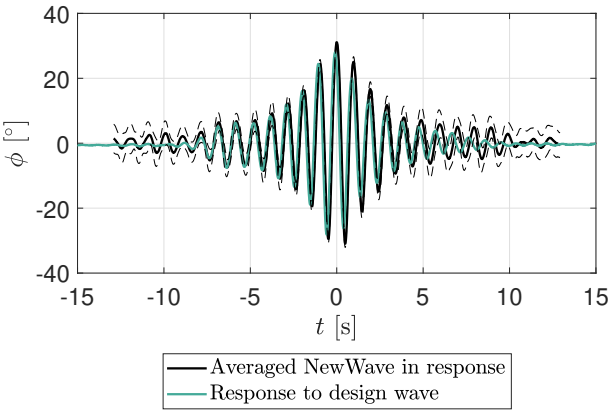

Fig. 9: Conditioned NewResponse (black solid) with error bars (dashed line, defined as $\pm 2\sigma/\sqrt{M}$) and response to Design Wave (turquoise)

the overall response level matches the sought response level well. We observe that the measured response period is slightly shorter than that of the averaged NewWave signal. The cause of this discrepancy is may be due to the difference between the surge response corresponding to a NewResponse and the measured surge response from the Design Wave test. This is because a rapid surge impulse at the passing of the Design Wave sequence will reduce the encounter wave speed at the centre floats. This phenomenon occurs both in the irregular waves and single wave group tests, however from two different initial positions, and it is therefore not straightforward to determine the effect.

For the response to the Design Wave at $t < 0$ s, the measured wave group matches θ^{NW} quite well, showing that the good match of the Design Wave observed at $t < 0$ s in Fig. 8 causes a likewise good match of the response. At the response trough at $t = -0.6$ s, the measured response amplitude is 4% smaller than the trough amplitude of the NewResponse, which is well within the error margins. At the following response peaks, the deviation of the crest and trough amplitude relative to the NewResponse increases to $\approx$ 20% for

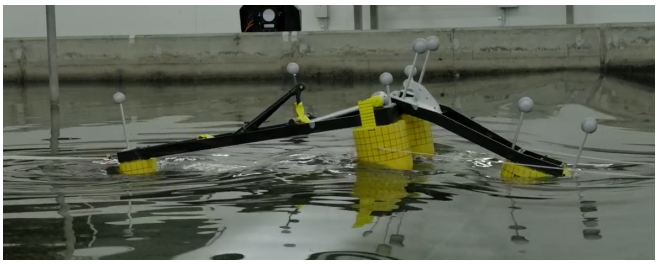

Fig. 10: Photo of the float at the main hinge-up crest at $t = 0$. Measured during the Design Wave test.

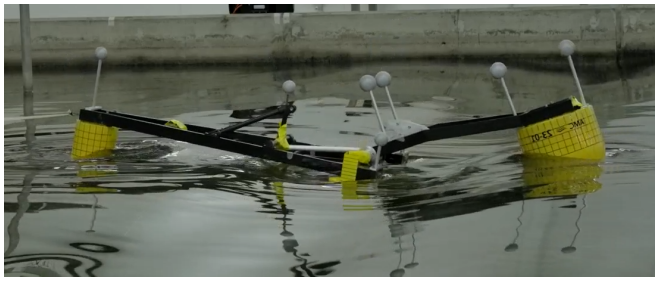

Fig. 11: Photo of the float at $t = -0.6$ s, at the hinge rotation trough immediately before the biggest response crest. Measured during the Design Wave test.

the following five response crests, which follows the curve of the lower error margin for the averaged NewResponse. A photo of the M4 device taken at $t = 0$ s during the Design Wave test is shown in Fig. 10, showing the top of the bow and stern floats close to the water surface, and the large angular displacement of the hinge. The stern float is mostly submerged at $t = 0$ s, and it appears that water is flowing onto the top of the float.

From video analysis of the Design Wave test, it was discovered that the centre floats were fully submerged at the response troughs preceding and following the largest response crest. Photographs of these instances are shown in Fig. 11 and Fig. 12.

Fig. 11 shows the response trough immediately before the maximum response. We observe partial submersion of the beam connecting the centre floats and green water over-topping the centre floats from the rear. This submersion process is what has previously been called dunking, which was observed in focused wave group tests of the M4 in Santo et al. [1]. Dunking was analysed in great detail and proved to drastically reduce the maximum measured response compared to linear estimates, but without affecting the subsequent decay rate of the response by linear radiation damping. They also observed self-collision of the centre float with the beam running to the stern float in conjunction or just before the dunking occurrence. During our experiments, we observed no such collision between the two parts, as the design of the M4 has been updated and improved since. However, we believe that the deviation of the measured response to the Design Wave compared to the averaged largest response is due to instantaneous damping exhibited during the submersion of the centre floats.

Although the submersion of floats is a highly non-

Fig. 12: Photo of the float at $t = 0.4$ s, at the hinge rotation trough immediately after the biggest response crest. Measured during the Design Wave test.

linear process, we have achieved a reasonable match between the response to the Design Wave with the averaged NewResponse despite the dunking events. This may be due to dunking events in the M averaged response signals. We will analyse this in detail in future work.

IV. Discussion

Hinge rotation of the M4 WEC in extreme waves has been analysed experimentally with a full Design Wave analysis. The largest average hinge-up motion was extracted from a long realisation of an irregular time series and subsequently reproduced experimentally by means of a Design Wave run as an isolated short-duration wave group. Both the Design Wave and NewResponse were successfully reproduced, with matching phase and amplitude mostly within $\pm 2\sigma/\sqrt{M}$ of the sought values. This serves as a proof that NewWave type Design Wave analysis works for predominantly linear narrow-banded responses, and encourages us to undertake further work to validate the method for more complex sea states and response processes.

Since the peak spreading measured in the King George Sound is 32° during summer months (Kurniawan et al. [6]), it is of interest to conduct Design Wave tests in spread seas, to account for any coupling effects which might occur. Numerical analysis of the M4 in extreme spread seas [1], [11] has shown only a small reduction in the maximum hinge rotation in bimodal seas compared to unidirectional. However, with the slender 1-2-1 design, compared to the analysed 1-3-2 design, differences e.g. a decrease in the roll moment of inertia might alter the behaviour in oblique and spread waves.

In the Design Wave test, the model experienced two instances of dunking - full submersion and over-topping of the centre floats. The dunking phenomenon was observed in NewWave tests by Santo et al. [1], but a detailed investigation of causes and impacts of the event was not possible with their data. With access to several hours of random extreme wave response from the AMC tests, we have the opportunity to study the conditions that cause dunking and the effect on the response. We plan to ultimately incorporate this knowledge in a numerical quasi-linear time-domain model.

As the Design Wave analysis is carried out based on long realisations of irregular sea states measured in a model test basin, some reflection by the beach can be expected (particularly for longer waves). However, since the extreme sea state was fairly steep, we expect wave breaking at the beach to quite effectively damp wave components in the linear frequency range. Since the peak frequencies of the wave and response spectrum are similar (see Fig. 4), the wave components which are of most consequence to the response are expected to be damped most effectively by the beach. In the Design Wave tests, the duration is short enough that any reflected wave group arrives several seconds after the last response to the Design Wave sequence has died out. Given the good match between the conditioned Design Wave and the measured Design Wave and the NewResponse and the measured response to the Design Wave respectively, we expect that the effect of wave reflection by the beach on extreme waves and responses is small. Further quantifying will be part of future work.

As mentioned, the surge response is expected to have an effect on Design Wave tests. In the long realisations of the extreme sea state, the soft mooring line gives a mean surge response, which is distinct from the still-water equilibrium position. Since the Design Wave tests conducted in the basin were not embedded in an irregular wave time series (as described by Taylor, Jonathan and Harland [20]) but were run in the form of a single isolated wave group, potential issues regarding the focal position of the Design Wave could arise. Although small, given the good match of the measured hinge response with the NewResponse, the effect of the surge response on the Design Wave will also be investigated in future work.

V. CONCLUSIONS

In this paper we presented an experimental analysis of extreme response of the M4 wave energy converter. This was carried out as a two-step conditioning NewWave type Design Wave analysis of the hinge rotation.

Part one consisted of a wave-by-wave conditioning analysis of the response using a long irregular wave realisation of a severe sea state, from which we identified a short Design Wave sequence using a NewWave conditioning analysis. We showed that the average shape of the largest response sequence is highly resonant with a build-up period spanning > 5 s and a free-decay period of similar duration. The whole process is highly symmetric.

In part two, the identified Design Wave sequence was run as an isolated short-duration wave group in the model test basin to validate the approach. We successfully reproduced the Design Wave surface elevation to a reasonable level of accuracy. We likewise showed that the hinge rotation response to the Design Wave matched the average largest response until the occurrence of the largest response crest. At the preceding and following troughs, full submersion and over-topping of the centre floats caused considerable dissipation of energy and resulted in a smaller than expected response in the free-decay phase.

The satisfactory reproduction of both the Design Wave and the averaged largest response in the sea state serves as validation of the conditioning Design Wave analysis approach. This highlights the opportunity to apply the Design Wave as input to high-fidelity modelling software such as Computational Fluid Dynamics or structural Finite Element Modelling to obtain detailed pressure and stress distributions during the extreme response events. For the current M4 configuration and design, accurate prediction of centre beam slamming will provide valuable information about the structural performance of the M4 machine.

VI. ACKNOWLEDGEMENTS

Authors CLH and HW would like to thank Benhur Joseph Raju, Damon Howe, Nick Johnson and the Australian Maritime College at the University of Tasmania for help and good collaboration during the experiments.

VII. NOMENCLATURE

$H(\omega)$	Linear wave to response transfer function
H_s	Significant wave height
h	Water depth
M	Small number of large crests
N	Number of waves/response crests in sea state
$S(\omega)$	Variance density spectrum
T_p	Peak period
T_z	Zero up-crossing period
α	NewWave or NewResponse amplitude
γ	Peak enhancement factor
ζ	Scale coefficient
η	Surface elevation
η^{NW}	NewWave
$\eta\|\theta^{NW}$	Incident wave conditioned on the NewResponse
θ	Hinge response
θ^{NW}	NewResponse
$\theta\|\eta^{NW}$	Hinge response conditioned on the NewWave
λ_p	Peak wavelength
λ_z	Zero up-crossing wave length
ξ	M4 rigid-body motion
σ	Standard deviation
ω	Angular frequency

REFERENCES

[1] H. Santo, P. H. Taylor, E. Carpintero Moreno, P. Stansby, R. Eatock Taylor, L. Sun, and J. Zang, "Extreme motion and response statistics for survival of the three-float wave energy converter M4 in intermediate water depth," *Journal of Fluid Mechanics*, vol. 813, pp. 175–204, 2 2017.

[2] J. R. Grice, P. H. Taylor, and R. Eatock Taylor, "Near-trapping effects for multi-column structures in deterministic and random waves," *Ocean Engineering*, vol. 58, pp. 60–77, 2013. [Online]. Available: http://dx.doi.org/10.1016/j.oceaneng.2012.09.021

[3] W. Zhao, P. Taylor, and H. Wolgamot, "Design waves and statistics of linear gap resonances in random seas," *Flow*, vol. 1, p. E11, 2021.

[4] W. Zhao, P. H. Taylor, H. A. Wolgamot, and R. Eatock Taylor, "Identifying linear and nonlinear coupling between fluid sloshing in tanks, roll of a barge and external free-surface waves," *Journal of Fluid Mechanics*, vol. 844, pp. 403–434, 6 2018.

[5] L. F. Chen, P. H. Taylor, D. Z. Ning, P. W. Cong, H. Wolgamot, S. Draper, and L. Cheng, "Extreme runup events around a ship-shaped floating production, storage and offloading vessel in transient wave groups," *Journal of Fluid Mechanics*, vol. 911, 2021.

[6] A. Kurniawan, H. Wolgamot, C. Gaudin, C. Shearer, P. Stansby, and B. Saunders, "Numerical modelling in the development of the M4 prototype for Albany, Western Australia," in *Proc. of the AMSE 2023 42nd Int. Conf. on Ocean, Offshore and Arctic Engineering*. Melbourne Australia: ASME, 6 2023.

[7] P. Stansby, E. Carpintero Moreno, T. Stallard, and A. Maggi, "Three-float broad-band resonant line absorber with surge for wave energy conversion," *Renewable Energy*, vol. 78, pp. 132–140, 6 2015. [Online]. Available: http://creativecommons.org/licenses/by/4.0/

[8] P. Stansby, E. C. Moreno, and T. Stallard, "Capture width of the three-float multi-mode multi-resonance broadband wave energy line absorber M4 from laboratory studies with irregular waves of different spectral shape and directional spread," *Journal of Ocean Engineering and Marine Energy*, vol. 1, no. 3, pp. 287–298, 8 2015.

[9] E. Carpintero Moreno and P. Stansby, "The 6-float wave energy converter M4: Ocean basin tests giving capture width, response and energy yield for several sites," *Renewable and Sustainable Energy Reviews*, vol. 104, pp. 307–318, 4 2019.

[10] J. Orszaghova, S. Lemoine, H. Santo, P. H. Taylor, A. Kurniawan, N. McGrath, W. Zhao, and M. V. Cuttler, "Variability of wave power production of the M4 machine at two energetic open ocean locations: Off Albany, Western Australia and at EMEC, Orkney, UK," *Renewable Energy*, vol. 197, pp. 417–431, 9 2022.

[11] H. Santo, P. H. Taylor, and P. K. Stansby, "The performance of the three-float M4 wave energy converter off Albany, on the south coast of western Australia, compared to Orkney (EMEC) in the U.K." *Renewable Energy*, vol. 146, pp. 444–459, 2 2020. [Online]. Available: https://doi.org/10.1016/j.renene.2019.06.146

[12] P. S. Tromans, A. R. Anaturk, and P. Hagemeijer, "A new model for the kinematics of large ocean waves - application as a design wave," in *Proceedings of the First (1991) International Offshore and Polar Engineering Conference*. The International Society of Offshore and Polar Engineers, 1991, pp. 64–71.

[13] G. Lindgren, "Some Properties of a Normal Process Near a Local Maximum on JSTOR," *The Annals of Mathematical Statistics*, vol. 41, no. 6, 1970. [Online]. Available: https://www.jstor.org/stable/2240325?seq=1

[14] P. Boccotti, "Some new results on statistical properties of wind waves," *Applied Ocean Research*, vol. 5, no. 3, pp. 134–140, 7 1983.

[15] J. N. Newman, *Marine Hydrodynamics*, 10th ed. The MIT Press, 1977.

[16] J. R. Grice, P. H. Taylor, and R. Eatock Taylor, "Second-order statistics and 'designer' waves for violent free-surface motion around multi-column structures," *Philosophical Transactions of the Royal Society A: Mathematical, Physical and Engineering Sciences*, vol. 373, no. 2033, 1 2015.

[17] W. Zhao, P. H. Taylor, H. A. Wolgamot, and R. Eatock Taylor, "Amplification of random wave run-up on the front face of a box driven by tertiary wave interactions," *Journal of Fluid Mechanics*, vol. 869, pp. 706–725, 6 2019.

[18] L. Chen, P. H. Taylor, S. Draper, H. Wolgamot, I. A. Milne, and J. R. Whelan, "Response based design metocean conditions for a permanently moored FPSO during tropical cyclones: Estimation of greenwater risk," *Applied Ocean Research*, vol. 89, pp. 115–127, 8 2019.

[19] D. Howe, B. J. Raju, C. L. Hansen, H. Wolgamot, A. Kurniawan, J.-R. Nader, C. Shearer, and P. Stansby, "Basin testing of the 1-2-1 M4 WEC," in *European Wave and Tidal Energy Conf.*, Bilbao, Spail, 7 2023.

[20] P. H. Taylor, P. Jonathan, and L. A. Harland, "Time domain simulation of jack-up dynamics with the extremes of a gaussian process," *Journal of Vibration and Acoustics, Transaction of the ASME*, vol. 119, pp. 624–628, 1997.